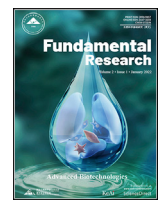


Contents lists available at ScienceDirect



Fundamental Research

journal homepage: <http://www.keaipublishing.com/en/journals/fundamental-research/>

Article

Unexpected type-II multiferroic phase in GdMnO_3 under high magnetic fieldsMing Yang ^{a,1}, Jun Chen ^{b,1}, Junfeng Wang ^{a,*}, Chao Dong ^a, Chengliang Lu ^a, Gang Xu ^a, Jinguang Cheng ^c, Jianshi Zhou ^d, Shuai Dong ^{b,*}^a Wuhan National High Magnetic Field Center and School of Physics, Huazhong University of Science and Technology, Wuhan 430074, China^b Key Laboratory of Quantum Materials and Devices of Ministry of Education, School of Physics, Southeast University, Nanjing 211189, China^c Beijing National Laboratory for Condensed Matter Physics and Institute of Physics, Chinese Academy of Sciences, Beijing 100190, China^d Materials Science and Engineering Program, Mechanical Engineering, University of Texas at Austin, Texas 78712, United States

ARTICLE INFO

Article history:

Received 24 June 2025

Received in revised form 9 December 2025

Accepted 16 December 2025

Available online xxx

Keywords:

Pulsed high magnetic field

Type-II multiferroic

Perovskite manganites

Magnetoelectric phase diagram

Spin-lattice coupling

ABSTRACT

Perovskite manganites with small A-site ions, as the first and canonical branch of type-II multiferroics, are ideal systems to exhibit magnetism-induced ferroelectricity. Despite their established magnetoelectric phase diagrams under low magnetic fields, here an unidentified phase with a large magnetism-induced polarization (up to 1500 $\mu\text{C}/\text{m}^2$) is revealed in GdMnO_3 under high magnetic fields up to 60 T. Based on multiprobe experiments, a complete phase diagram is constructed with successive polar-nonpolar-polar-nonpolar transitions. Such a non-monotonic evolution is well mimicked by model simulation, while the spin-lattice coupling is the key ingredient for the reentrant ferroelectric phase.

1. Introduction

Orthorhombic rare-earth manganites, with general formulas RMnO_3 and RMn_2O_5 , set off an intense period of interest in type II multiferroics [1,2], which co-establish a fertile playground to explore the multiferroicity and colossal magnetoelectricity [3–6]. As canonical type-II multiferroics, their special physical properties have been systematically revealed, and more importantly their magnetoelectric mechanisms also shed light on the whole field of multiferroics [7–10].

Although tremendous interests have been drawn to investigate the complex magnetic orders and related ferroelectricity in these systems [11–15], unexpected magnetoelectric states/behaviors with new physics are continually emerging. For example, very recently, GdMn_2O_5 was reported to exhibit a topologically protected switching phenomenon, that a four-state polarization flop is realized at a magic angle under strong magnetic fields [16,17].

In contrast to the complicated RMn_2O_5 , RMnO_3 's are relative simpler regarding its crystalline and magnetic structures, which have been generally understood as follows. For those relative large R ions, e.g. La^{3+} and Pr^{3+} , the ground state of RMnO_3 is A-type antiferromagnetic

(A-AFM), which is not ferroelectric [18,19]. Weak ferromagnetism also occurs from the spin canting. For those middle-size R^{3+} 's, e.g. Tb^{3+} and Dy^{3+} , the magnetic ground states become the cycloid spiral (SP) ones [11,12,19], which induce polarizations (in the order of $\sim 1000 \mu\text{C}/\text{m}^2$) via the inverse Dzyaloshinskii-Moriya interaction (DMI) [20,21]. For those small-size R^{3+} 's, e.g. Ho^{3+} and Lu^{3+} , the magnetic order at low temperatures is E-type antiferromagnetic (E-AFM), which can generate large polarizations in the order of $\sim 5000 - 10000 \mu\text{C}/\text{m}^2$ via the exchange striction mechanism [22,23]. Such a phase evolution as a function of R^{3+} size can be well reproduced by the double-exchange model or classical spin model [24–27], both of which rely on the subtle competition between the nearest-neighbor and next-nearest-neighbor interactions.

For those compounds near phase boundaries, the magnetoelectric behaviors can be nontrivial. For example, for $R = \text{Eu}$, there is a field-induced ferroelectric SP phase under high magnetic fields $22 \text{ T} < H < 50 \text{ T}$, although its zero-field ground state is paraelectric and A-AFM (and weakly ferromagnetic) [28]. Similar behavior was also reported for GdMnO_3 with a much lower threshold of magnetic field ($\sim 1 \text{ T}$), since it is very proximate to the boundary between the A-AFM and SP phases

^{*} Corresponding authors.E-mail addresses: jfwang@hust.edu.cn (J. Wang), sdong@seu.edu.cn (S. Dong).¹ These authors contributed equally to this work.<https://doi.org/10.1016/j.fmre.2025.12.014>2667-3258/© 2025 The Authors. Publishing Services by Elsevier B.V. on behalf of KeAi Communications Co. Ltd. This is an open access article under the CC BY-NC-ND license (<http://creativecommons.org/licenses/by-nc-nd/4.0/>)

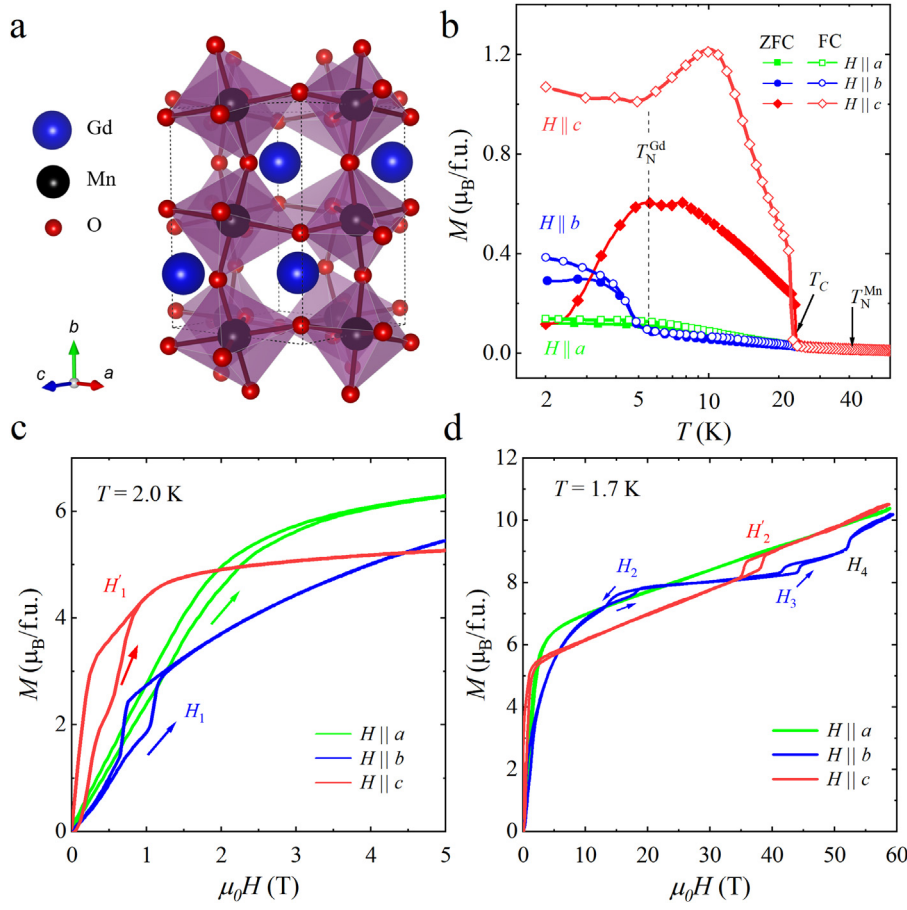


Fig. 1. Magnetization M for magnetic field along different crystalline axes at 1.7 K. The inset shows M at low field range which are measured by SQUID at 2 K. The arrows indicate the sweeping direction of magnetic fields.

[12]. Then is the magnetoelectric story of $RMnO_3$'s fully completed after their history of two decades?

In this work, a systematic high-field study is performed on $GdMnO_3$ single crystals. With pulsed fields up to 60 T, a hidden magnetoelectric phase is uncovered in the high-field region. A novel polar-nonpolar-polar-nonpolar transition sequence occurs with increasing magnetic field. And the phase diagram can be mimicked by a spin model with multiple interactions, which predicts an orthogonal spin stripe phase as the second polar phase. The spin-lattice coupling is the key ingredient for the multiferroicity of new phase.

2. Methods

Single crystals were grown by the floating-zone method as described elsewhere [29]. Crystals were orientated by the Laue X-ray photography and cut into cubes with dimensions $2\text{ mm} \times 2\text{ mm} \times 2\text{ mm}$ for magnetization measurements and plates $2\text{ mm} \times 2\text{ mm} \times 0.2\text{ mm}$ for electric polarization and magnetostriction measurements, respectively. High magnetic field measurements were performed in a 12 ms-pulsed magnet at Wuhan National High Magnetic Field Center. The magnetization was measured by the induction method using a coaxial pickup coil and calibrated by the low-field data measured by a superconducting quantum interference device (Quantum Design SQUID). The electric polarization was probed by measuring and integrating the pyroelectric current flowing through the two largest surfaces of a platelike sample with electrodes attached by silver paste [30,31]. During the polarization measurements, a bias voltage of 100 V, which converts into a bias field of $E = +500\text{ kV/m}$, was applied to polarize the FE domains induced by external magnetic fields. Magnetostriction along the

field direction was measured by the fiber-Bragg-grating (FBG) method [32].

3. Experimental results

Fig. 1 shows the magnetization (M) along the crystallographic a , b , and c axes of $GdMnO_3$ at 1.7 K. The low field results, as shown in the inset of **Fig. 1** and Fig. S1 in Supplementary Materials (SM) [33], are consistent with previous reports [12,34], which indicate the c -axis as the macroscopic easy magnetization axis. Since the ground state of $GdMnO_3$ is antiferromagnetic, the microscopic easy axis of spins should be perpendicular to the easy magnetization axis, i.e., lying in the ab plane. Remarkable hysteresis behaviors between the increasing and decreasing fields are discernible under 3 T along all directions, indicating a first-order transition in the low-field region. As reported before, this transition was attributed to the A-AFM to SP phase transition.

For $H \parallel a$, M steeply increases up to $\sim 6\text{ }μ_B$ per formula unit (f.u.) at 3 T and then rises linearly without any anomaly nor saturation till the maximum field. Due to the very localized electronic cloud of $4f$ orbitals, the nearest neighboring exchanges between $4f - 4f$ spins (as well as between $4f - 3d$ spins) are naturally weak (usually $< 1\text{ meV}$). Thus the magnetic moments of Gd^{3+} are much easier to be aligned ferromagnetically by external magnetic field. Noting that the saturated moments of Gd^{3+} and Mn^{3+} are $7\text{ }μ_B$ and $4\text{ }μ_B$, respectively. Then the low-field steep increase of magnetization can only be mainly attributed to the parallel alignment of Gd^{3+} spins. The slightly reduced magnetization from the saturation value ($7\text{ }μ_B$ per f.u.) is due to the antiparallel contribution from Mn^{3+} 's canting spins [34].

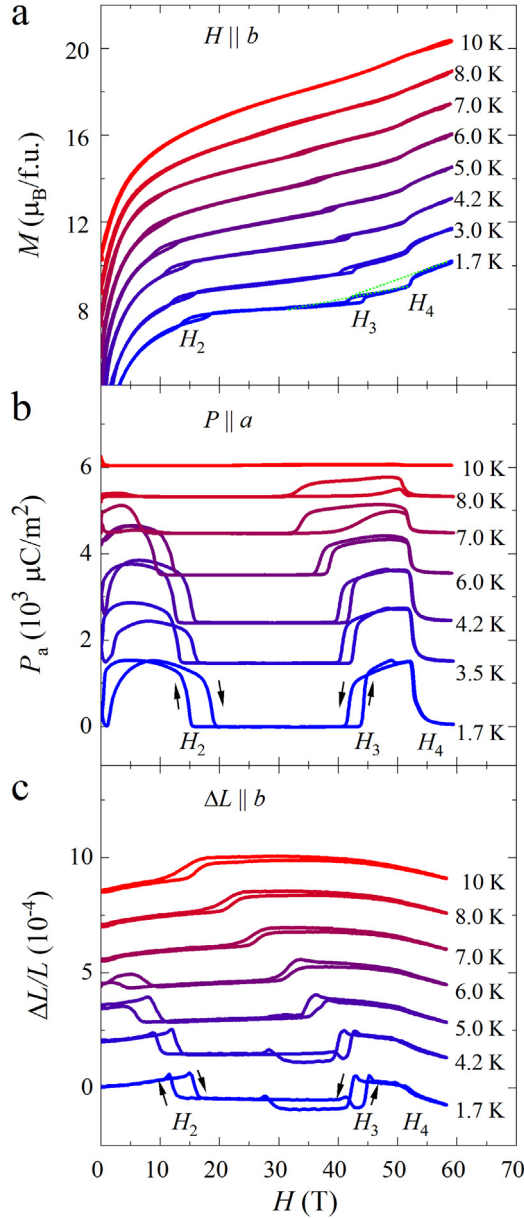


Fig. 2. (a) Magnetization M , (b) polarization P_a , and (c) magnetostriction $\Delta L/L$ along the b -axis at various temperatures for $H \parallel b$ up to 60 T. All curves are vertically shifted for clarity.

In contrast to the featureless magnetization vs field curves of $H \parallel a$, a series of successive magnetic transitions are found at $H_1 \sim 0.6$ T, $H_2 \sim 14$ T, $H_3 \sim 41$ T, and $H_4 \sim 52$ T for $H \parallel b$. The first three transitions at H_1 , H_2 , and H_3 are all in the first-order, characterized by the presence of hysteresis loops. However, the hysteresis at H_4 becomes immeasurably small and thus this transition is likely second order at the measured temperatures. Interestingly, an approximative plateau of magnetization is observed between H_2 and H_3 , indicating a gaped state in this range.

For comparison, when H is applied along the c axis, only another spin-flip transition can be found at $H'_2 \sim 35$ T, in addition to the first one at $H'_1 \sim 0.8$ T. Furthermore, the two $M - H$ curves of the $H \parallel a$ and $H \parallel c$ cases coincide with each other when $H > H'_2$, implying the magnetic isotropy in the ac plane above this field. Another conclusion is that a full saturation magnetization ($11 \mu_B/\text{f.u.}$) has not been reached till 60 T, although it is indeed approached ($> 10 \mu_B/\text{f.u.}$). As stated before, since Gd^{3+} 's spins are almost fully aligned ferromagnetically above 3 T,

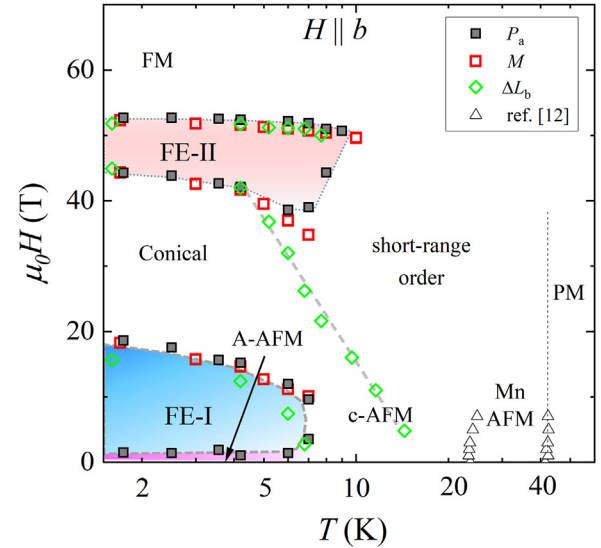


Fig. 3. The magnetoelectric phase diagram of GdMnO_3 . Circles and squares denote the transition fields on the $M(H)$ and $P(H)$ curves. Open and filled symbols represent the increasing and decreasing field, respectively. Open triangles are extracted from ref. [12].

these high-field transitions should be attributed to the re-ordering of the Mn^{3+} 's spins.

The successive anomalies in the b -axis magnetization indicate the unknown magnetic transitions under high fields, which are beyond all previous reports and certainly deserve more investigations. The temperature dependence of $M - H$ curves are plotted in Fig. 2a. First, with increasing temperature, all anomalies become weaker and weaker and finally disappear at around 8 K. Second, both the transitions at H_2 and H_3 move towards lower fields, while the transition at H_4 persists without obvious shifting.

To reveal more information of these high-field transitions of GdMnO_3 , the electric polarization along the a -axis (P_a) is measured as a function of $H \parallel b$, as shown in Fig. 2b. It is clear that a non-monotonic evolution of P_a with multiple steps coincides well with the M curves [Fig. 2a]. At $T = 1.7$ K, a finite P_a emerges rapidly since H_1 , consistent with previous reports [12,35], which was successfully ascribed to the field-induced ab -plane cycloidal structure of Mn^{3+} spins. Unexpectedly, this P_a decreases to zero at H_2 and the system restores to the paraelectric state till H_3 . Even more surprisingly, the P_a emerges again in the high-field region between H_3 and H_4 , and the paraelectric state restores again beyond H_4 . Such a nontrivial evolution defines five phases. As aforementioned, the first two below H_2 had been understood and the last one beyond H_4 is almost ferromagnetic. Then the rest two between H_2 and H_4 should be clarified.

The magnitude of high-field P_a is comparable to the low-field one, reaching $\sim 1500 \mu\text{C}/\text{m}^2$. Hystereses of P_a exist at H_1 , H_2 , and H_3 , while non-hysteresis occurs at H_4 . These behaviors, as well as the their temperature-dependences, coincide with aforementioned $M - H$ curves.

The magnetostriction $\Delta L/L$ along b -axis is also characterized. As shown in Fig. 2c, at $T = 1.7$ K, the transition fields, plateaus, and hystereses of $\Delta L/L$ generally match well with the behaviors of M and P_a . Another interesting behavior is that the hystereses of $\Delta L/L$ are broader, which even persist at relative high temperatures (e.g. 10 K). These differences between magnetostriction and polarization may come from the complex domain dynamics during those first-order transitions.

In summary of experimental results, the spin re-ordering under high fields are responsible for the non-monotonic evolution of P_a . Based on above results, a magnetoelectric phase diagram of GdMnO_3 is sketched in Fig. 3, while the phase boundaries are defined by aforementioned transitions.

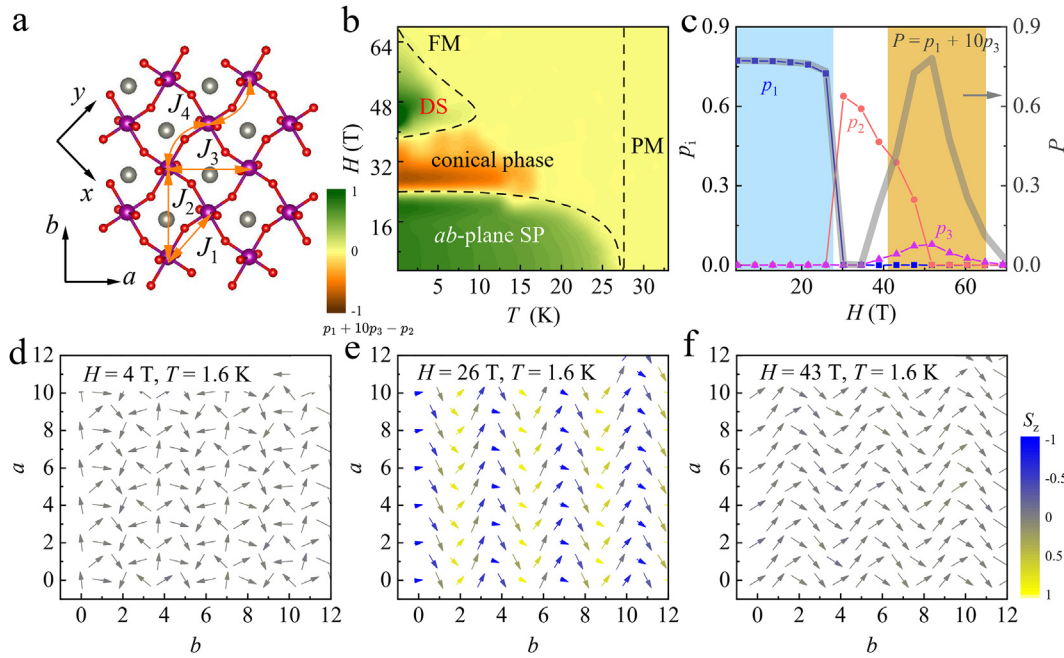


Fig. 4. (a) Top view of GdMnO_3 in ab -plane and labelled exchange interaction J_1 , J_2 , J_3 and J_4 . (b) Phase diagram in T – H space with color contour map determined by the value $p_1 + 10p_3 - p_2$; (c) The evolution of order parameters $p_1 = \langle |\sum_{i,\hat{u}=\langle x,\hat{u} \rangle} \mathbf{S}_i \cdot (\mathbf{S}_i - \mathbf{S}_{i+\hat{u}})| \rangle / 4N$, $p_2 = \langle |\sum_{i,\hat{u}=\langle x,\hat{u} \rangle} \hat{u} \cdot (\mathbf{S}_i \times \mathbf{S}_{i+\hat{u}})| \rangle / 2N$, $p_3 = \langle |\sum_{i,\hat{u}=\langle x,\hat{u} \rangle} \hat{u} \cdot (\mathbf{S}_i \times \mathbf{S}_{i+\hat{u}})| \rangle / 2N$ and the weighted parameter P at low temperature (1.6 K) as functions of magnetic field. (c-e) The ab -plane spiral phase (SP). (d) The conical phase. (e) The orthogonal antiferromagnetic double stripes (DS) phase. Only in the conical phase, the out-of-plane spin components are nonzero, as indicated by the color contour map.

4. Model simulations and discussion

Although the reentrances of multiferroic phases under high magnetic fields have already been observed in other frustrated magnetic systems like $\text{Ni}_3\text{V}_2\text{O}_8$, $\text{A}_2\text{V}_2\text{O}_7$ ($\text{A}=\text{Ni, Co}$), and CuCrO_2 [30,36–39], their underlying mechanisms seem to be unambiguously different. The magnitude of these high-field polarization is in the order of $100 \mu\text{C}/\text{m}^2$ or even smaller, which should be originated from the inverse DMI and field-induced SP phases. In other words, the reentrant multiferroic phases in those systems are more similar to the first multiferroic phase in GdMnO_3 . Therefore, the high-field multiferroic phase in GdMnO_3 , with a much larger polarization up to $1500 \mu\text{C}/\text{m}^2$, should be understood with an alternative scenario.

In the current stage, the common techniques to directly characterize magnetic orders, like neutron scattering, are not available under such high magnetic fields. Thus, a model simulation becomes the preferred approach to access more details of the high-field phase. In fact, Mochizuki et al. developed a classical spin model for RMnO_3 's [25,26,40,41], which can precisely describe their complex phase diagram in the low-field region. Based on Mochizuki et al.'s model, a simplified model Hamiltonian is used here:

$$H = \sum_{i,j} J_n \mathbf{S}_i \cdot \mathbf{S}_j - J_b \sum_{i,j} (\mathbf{S}_i \cdot \mathbf{S}_j)^2 + \sum_i [A_c (S_i^z)^2 - A_\delta (S_i^z)^4] - J_\delta \sum_i \sum_{u=x,y} (\mathbf{S}_i \cdot (\mathbf{S}_{i+u} - \mathbf{S}_{i-u}))^2 + \mathbf{H} \cdot \sum_i \mathbf{S}_i, \quad (1)$$

where the first is the neighboring exchanges between Mn's spins (\mathbf{S} 's), including in-plane $J_1/J_2/J_3/J_4$ [see Fig. S5(a)] and out-of-plane J_c . The second term is biquadratic interaction merely for the nearest neighboring spins. The third term includes conventional single-ion anisotropy and cubic anisotropy. The fourth term is an effective expression for spin-lattice coupling (i.e. the exchange striction), which prefers the E-AFM order. The last one is Zeeman energy under magnetic field \mathbf{H} along b direction. In our model, only Mn's sublattice is considered, thus the low-field magnetic phase (below 2 T) could not be interpreted while Gd's sublattice is only a ferromagnetic background.

We apply first-principles calculations to determine the realistic relationship among all the exchange interactions, then with proper coefficients choice and using Monte Carlo simulations [more details refer to SM [33]], the phase diagram can be well reproduced (even not every detail), as shown in Fig. 4b. The phase regions are determined by the order parameters, as shown in Fig. 4c. According to our simulations, at low temperatures and in the low-field region, the magnetic state is belonging to the ab -plane spiral phase with incommensurate modulation vector $q \approx 0.27$ as performed in Fig. 4d, which almost matches the previous experimentally measured $q = 1/4$ [12]. With increasing magnetic field, the system turns to be the conical phase [Fig. 4e]. Further increasing field, the spin texture forms special orthogonal antiferromagnetic double stripes (DS), as characterized as “ $\uparrow\uparrow\uparrow\rightarrow\rightarrow\rightarrow$ ” lying in the ab plane [Fig. 4f], which generally breaks the inversion symmetry to become a novel promising FE phase. In fact, the DS order has already been suggested as a possible ground state in the earlier study [12] and also similar to a previously predicted “spin-orthogonal stripe” although not identical [42]. It's noteworthy that the presence of DS phase is significantly dependent on spin-lattice coupling with a certain strength [see Fig. S6b], rendering a subtle competition of magnetic phases. In addition, the mentioned phase transitions simultaneously contribute to the sudden change of magnetization as illustrated in Fig. S7, aligning with experiments well. For all these three orders, their modulation vectors are along the b -axis, and the interlayer coupling also changes from anti-ferromagnetic and ferromagnetic gradually. In the very high-field limit, the system finally becomes ferromagnetic.

The associated polarizations accompanying this magnetic evolution are also estimated. Here both the inverse DMI [$\sim \sum_{i,j} \mathbf{e}_{ij} \times (\mathbf{S}_i \times \mathbf{S}_j)$] [21], and the exchange striction [$\sim \sum_{i,u=x,y} (-1)^i [\mathbf{S}_i \cdot (\mathbf{S}_{i+u} - \mathbf{S}_{i-u})] \mathbf{v}$ ($v = y/x$)] [22], are considered for the generation of polarizations [33]. First, the ab -plane spiral phase can lead to a ferroelectric polarization along the a -axis, generated by the inverse DMI as expected. Second, the intermediate conical phase is nonpolar. Third, the orthogonal stripy phase restores the ferroelectricity along the a -axis, although the underlying mechanism is replaced by exchange striction. The polarization finally fades away in the high-field ferromagnetic phase. Typically, the

polarization produced by the spiral order is smaller than $\sim 0.1 \mu\text{C}/\text{cm}^2$, while the exchange striction mechanism dominated polarization can be up to $\sim 1 \mu\text{C}/\text{cm}^2$ [43,44]. As a reasonable simplification, a weighted parameter $P = p_1 + 10p_3$ is introduced to describe the evolution of polarization plotted in Fig. 4b, indicating both two FE phases probably host quantitatively similar values of polarization. In short, our model simulation indeed reproduces the reentrance of ferroelectricity, i.e. the nontivial polar-nonpolar-polar-nonpolar evolution as well as the possible hidden spin-orthogonal double stripy phase.

5. Conclusion

In summary, a hidden type-II multiferroic phase with possible orthogonal spin stripes and large polarization has been revealed in GdMnO_3 crystal under high magnetic fields. A full magnetoelectric phase diagram has been established, which is also well reproduced by the model simulation. The spin texture and associated magnetoelectric mechanism are totally different from other type-II multiferroics with reentrance under high field. Our study suggests that unexpected quantum states with multiferroicity may exist even in those well-studied prototype multiferroics.

Declaration of competing interest

The authors declare that they have no conflicts of interest in this work.

CRediT authorship contribution statement

Ming Yang: Writing – review & editing, Writing – original draft, Methodology, Investigation, Formal analysis, Data curation, Conceptualization. **Jun Chen:** Writing – original draft, Visualization, Software. **Junfeng Wang:** Writing – review & editing, Writing – original draft, Resources, Project administration, Methodology, Funding acquisition, Conceptualization. **Chao Dong:** Methodology, Formal analysis, Data curation. **Chengliang Lu:** Methodology, Conceptualization. **Gang Xu:** Writing – original draft, Validation, Software. **Jinguang Cheng:** Writing – original draft, Supervision, Resources, Funding acquisition. **Jianshi Zhou:** Writing – original draft, Supervision, Methodology. **Shuai Dong:** Writing – original draft, Supervision, Software, Project administration, Methodology.

Acknowledgments

This work is supported by the National Key Research and Development Plan Project of China (2024YFA1611200), the National Natural Science Foundation of China (12074135, 12004122, 11834002, 12474085, 12025408 and 11874400) and the Fundamental Research Funds for the Central Universities (2019kfyXJJ009). This work is also partly supported by the interdisciplinary program of Wuhan National High Magnetic Field Center (WHMFC202205 and WHMFC202504), Huazhong University of Science and Technology. We thank the Big Data Center of Southeast University for providing the facility support on the numerical calculations.

Supplementary material

Supplementary material associated with this article can be found, in the online version, at [10.1016/j.fmre.2025.12.014](https://doi.org/10.1016/j.fmre.2025.12.014)

References

- [1] T. Kimura, T. Goto, H. Shintani, et al., Magnetic control of ferroelectric polarization, *Nature* 426 (2003) 55–58.
- [2] N. Hur, S. Park, P.A. Sharma, et al., Electric polarization reversal and memory in a multiferroic material induced by magnetic fields, *Nature* 429 (2004) 392–395.
- [3] O. Prokhnенко, R. Feyerherm, E. Dudzik, et al., Enhanced ferroelectric polarization by induced Dy spin order in multiferroic DyMnO_3 , *Phys. Rev. Lett.* 98 (2007) 057206.
- [4] N. Aliouane, K. Schmalzl, D. Senff, et al., Flop of Electric Polarization Driven by the Flop of the Mn SpinCycloid in Multiferroic TbMnO_3 , *Phys. Rev. Lett.* 102 (2009) 207205.
- [5] M. Fukunaga, Y. Sakamoto, H. Kimura, et al., Magnetic-field induced polarization flop in multiferroic TmMn_2O_5 , *Phys. Rev. Lett.* 103 (2009) 077204.
- [6] N. Lee, C. Vecchini, Y.J. Choi, Giant tunability of ferroelectric polarization in GdMn_2O_5 , *Phys. Rev. Lett.* 110 (2012) 137203.
- [7] S.-W. Cheong, M. Mostovoy, Multiferroics: A magnetic twist for ferroelectricity, *Nat. Mater.* 6 (2007) 13–20.
- [8] Y. Tokura, S. Seki, N. Nagaosa, Multiferroics of spin origin, *Rep. Prog. Phys.* 77 (2014) 076501.
- [9] S. Dong, J.-M. Liu, S.W. Cheong, et al., Multiferroic materials and magnetoelectric physics: Symmetry, entanglement, excitation, and topology, *Adv. Phys.* 64 (2015) 519–626.
- [10] S. Dong, H.J. Xiang, E. Dagotto, Magnetoelectricity in multiferroics: A theoretical perspective, *Natl. Sci. Rev.* 6 (2019) 629–641.
- [11] M. Kenzelmann, A.B. Harris, S. Jonas, et al., Magnetic inversion symmetry breaking and ferroelectricity in TbMnO_3 , *Phys. Rev. Lett.* 95 (2005) 087206.
- [12] T. Arima, T. Goto, Y. Yamasaki, et al., Magnetic-field-induced transition in the lattice modulation of colossal magnetoelectric GdMnO_3 and TbMnO_3 compounds, *Phys. Rev. B* 72 (2005) 100102.
- [13] D. Senff, P. Link, K. Hradil, et al., Magnetic excitations in multiferroic TbMnO_3 : Evidence for a hybridized soft mode, *Phys. Rev. Lett.* 98 (2007) 137206.
- [14] E. Schierle, V. Soltwisch, D. Schmitz, et al., Cycloidal order of 4f moments as a probe of chiral domains in DyMnO_3 , *Phys. Rev. Lett.* 105 (2010) 167207, doi:10.1103/PhysRevLett.105.167207.
- [15] M. Schiebl, A. Shuvayev, A. Pimenov, et al., Order-disorder type critical behavior at the magnetoelectric phase transition in multiferroic DyMnO_3 , *Phys. Rev. B* 91 (2015) 224205.
- [16] L. Ponet, S. Artyukhin, T. Kain, et al., Topologically protected magnetoelectric switching in a multiferroic, *Nature* 607 (2022) 81–85.
- [17] H.W. Wang, F. Wang, M. Yang, et al., Observation of universal topological magnetoelectric switching in multiferroic GdMn_2O_5 , *Phys. Rev. Lett.* 134 (2025) 016708.
- [18] T. Kimura, S. Ishihara, H. Shintani, et al., Distorted perovskite with eg1 configuration as a frustrated spin system, *Phys. Rev. B* 68 (2003) 060403.
- [19] T. Goto, T. Kimura, G. Lawes, et al., Ferroelectricity and giant magnetocapacitance in perovskite rare-earth manganites, *Phys. Rev. Lett.* 92 (2004) 257201.
- [20] I.A. Sergienko, E. Dagotto, Role of the Dzyaloshinskii-Moriya interaction in multiferroic perovskites, *Phys. Rev. B* 73 (2006) 094434.
- [21] H. Katsura, N. Nagaosa, A.V. Balatsky, Spin current and magnetoelectric effect in noncollinear magnets, *Phys. Rev. Lett.* 95 (2005) 057205.
- [22] I.A. Sergienko, C. Sen, E. Dagotto, Ferroelectricity in the magnetic E-phase of orthorhombic perovskites, *Phys. Rev. Lett.* 97 (2006) 227204.
- [23] S. Ishiwata, Y. Kaneko, Y. Tokunaga, et al., Perovskite manganites hosting versatile multiferroic phases with symmetric and antisymmetric exchange strictions, *Phys. Rev. B* 81 (2010) 100411.
- [24] S. Dong, R. Yu, S. Yunoki, J.-M. Liu, et al., Origin of multiferroic spiral spin order in the RMnO_3 perovskites, *Phys. Rev. B* 78 (2008) 155121.
- [25] M. Mochizuki, N. Furukawa, Microscopic model and phase diagrams of the multiferroic perovskite manganites, *Phys. Rev. B* 80 (2009) 134416.
- [26] M. Mochizuki, N. Furukawa, N. Nagaosa, Theory of spin-phonon coupling in multiferroic manganese perovskites RMnO_3 , *Phys. Rev. B* 84 (2011) 144409.
- [27] S. Dong, J.M. Liu, Recent progress of multiferroic perovskite manganites, *Mod. Phys. Lett. B* 26 (2012) 1230004.
- [28] M. Tokunaga, Y. Yamasaki, Y. Onose, et al., Novel multiferroic State of $\text{Eu}_{1-x}\text{Y}_x\text{MnO}_3$ in high magnetic fields, *Phys. Rev. Lett.* 103 (2008) 187202.
- [29] J.-S. Zhou, J.B. Goodenough, Unusual Evolution of the Magnetic Interactions versus Structural Distortions in RMnO_3 Perovskites, *Phys. Rev. Lett.* 96 (2006) 247202.
- [30] R. Chen, J.F. Wang, Z.W. Ouyang, et al., Magnetic field induced ferroelectricity and half magnetization plateau in polycrystalline $\text{R}_2\text{V}_2\text{O}_7(\text{R}=\text{Ni}, \text{Co})$, *Phys. Rev. B* 98 (2018) 184404.
- [31] W.-X. Liu, R. Chen, Y.-J. Liu, et al., A pulsed high magnetic field facility for electric polarization measurements, *Acta Phys. Sin.* 69 (2020) 057502.
- [32] R. Daou, F. Weickert, M. Nicklas, et al., High resolution magnetostriction measurements in pulsed magnetic fields using fiber Bragg gratings, *Rev. Sci. Instrum.* 81 (3) (2010) 033909.
- [33] See Supplemental Material at [URL will be inserted by publisher] for additional information, which includes the basic magnetization and electric polarization properties along different directions, and the details of the Monte Carlo simulation.
- [34] J. Hemberger, S. Lobina, H.-A. Krug von Nidda, et al., Complex interplay of 3d and 4f magnetism in $\text{La}_{1-x}\text{Gd}_x\text{MnO}_3$, *Phys. Rev. B* 70 (2004) 024414.
- [35] T. Kimura, G. Lawes, T. Goto, et al., Magnetoelectric phase diagrams of orthorhombic RMnO_3 ($\text{R}=\text{Gd}, \text{Tb}$, and Dy), *Phys. Rev. B* 71 (2005) 224425.
- [36] E. Mun, M. Frontzek, A. Podlesnyak, et al., High magnetic field evolution of ferroelectricity in CuCrO_2 , *Phys. Rev. B* 89 (2014) 054411.
- [37] H. Mitamura, T. Sakakibara, H. Nakamura, et al., Multiferroicity on the zigzag-chain antiferromagnet MnWO_4 in high magnetic fields, *J. Phys. Soc. Jpn.* 81 (2012) 054705.
- [38] J.F. Wang, W.X. Liu, Z.Z. He, et al., Ferroelectric polarization reversal in multiferroic MnWO_4 via a rotating magnetic field up to 52 T, *Phys. Rev. B* 104 (2021) 014415.
- [39] C. Dong, J.F. Wang, Z.Z. He, et al., Reentrantferroelectric phase induced by a tilting high magnetic field in $\text{Ni}_3\text{V}_2\text{O}_8$, *Phys. Rev. B* 105 (2022) 024427.

- [40] M. Mochizuki, N. Furukawa, Theory of magnetic switching of ferroelectricity in spiral magnets, *Phys. Rev. Lett.* 105 (18) (2010) 187601, doi:[10.1103/physrevlett.105.187601](https://doi.org/10.1103/physrevlett.105.187601).
- [41] M. Mochizuki, N. Furukawa, N. Nagaosa, Spin model of magnetostrictions in multiferroic Mn perovskites, *Phys. Rev. Lett.* 105 (2010) 037205.
- [42] S. Dong, R. Yu, J.-M. Liu, et al., Striped multiferroic phase in double-exchange model for quarter-doped manganites, *Phys. Rev. Lett.* 103 (2009) 107204.
- [43] R. Valdés Aguilar, M. Mostovoy, A.B. Sushkov, et al., Origin of electromagnon excitations in multiferroic RMnO_3 , *Phys. Rev. Lett.* 102 (2009) 047203.
- [44] T. Aoyama, K. Yamauchi, A. Iyama, et al., Giant spin-driven ferroelectric polarization in TbMnO_3 under high pressure, *Nat. Commun.* 5 (1) (2014) 4927.

Author profile

Ming Yang (BRID: [07227.00.81070](https://orcid.org/07227.00.81070)) is an associate professor in the Wuhan National High Magnetic Field Center (WHMFC), Huazhong University of Science and Technology. He obtained his PhD from the Laboratoire National des Champs Magnétiques Intenses (LNCMI) in Toulouse, France, and joined WHMFC in 2018. His research interests mainly focus on exploring the magnetic characteristics of different material systems, such as multiferroics, superconductors and charge density wave compounds.

Junfeng Wang (BRID: [09668.00.26218](https://orcid.org/09668.00.26218)) is a professor, PhD supervisor and deputy director of the Wuhan National High Magnetic Field Center (WHMFC), Huazhong University of Science and Technology. He obtained his PhD in 2006 from the Department of Physics, Wuhan University. After completing the postdoctoral work in the international MegaGauss Science Laboratory of the University of Tokyo, he joined the current university. His research interests mainly focus on multiferroics and strongly correlated electrons employing various measurement techniques in pulsed high magnetic fields.

Shuai Dong (BRID: [09775.00.89399](https://orcid.org/09775.00.89399)) is a Chair Professor at Southeast University, where he currently serves as the Chair of the School of Physics. As a theorist, his main research interests focus on quantum materials, especially those exhibiting ferroic properties. He received his PhD degree from Nanjing University and studied/worked as a visiting student, and later as a visiting assistant professor/scientist, at the University of Tennessee at Knoxville and Oak Ridge National Laboratory. He is a recipient of NSFC Distinguished Young Scholars. Prior to joining the Editorial Board of *PRL*, he served as an associate editor for *NPJ Quantum Materials*.